J Appl Electrochem (2014) 44:1239–1251
DOI 10.1007/s10800-014-0746-3

RESEARCH ARTICLE

Voltammetry of nanoparticle-coupled imine linkage-based receptors for sensing of Al(III) and Co(II) ions

Susheel K. Mittal · Rashmi Sharma · Manisha Sharma · Narinder Singh · Jasminder Singh · Navneet Kaur · Manmohan Chhibber

Received: 22 May 2014 / Accepted: 3 September 2014 / Published online: 13 September 2014

Abstract Zinc oxide nanoparticle-coupled imine linkage-based receptors (*T4*, *T5* and *T6)* were studied for their voltammetric characteristics. *T4* and *T5* having electron withdrawing and electron donating substituents at meta position of the imine linkage showed prominent cathodic (reduction of imine group) peaks at −0.930 and −1.850 V, respectively, while *T6* (without any substituent) showed a cathodic peak at −1.220 V. Voltammograms of the receptors indicated that *T4* and *T5* responded quantitatively for aluminium ions, while *T6* responded for cobalt ions. All the three receptors exhibited linear dynamic concentration ranges between 0.1 and 0.42 μM with regression coefficients ≥0.98. Calibration curves for the determination of aluminium and cobalt ions based on DPV data are reported and supported with potentiometric studies. Energy minimization studies using Gaussian 03W software also supported stability of the complexes. The proposed analytical method has been validated with complexometric method for metal detection in real-time samples.

Keywords ZnO nanoparticle-coupled imine-based receptors · Voltammetric sensor · Aluminium/cobalt detection · Theoretical study · Substituent effects

1 Introduction

Studies on electrochemical reduction of imine linkage [1–3] have always been important for analytical chemists as the charge distribution over the imine bond can be influenced easily by substitutions at position—meta to the imine linkage. This redistribution of electron density results in shift of cathodic peaks by significant potentials which forms the basis of sharp chemical sensing using receptors based on imine linkages. Further doping with ZnO nanoparticles is found to affect grain boundaries [4, 5] and hence influence redox characteristics of the parent compound [6]. The imine-linked receptor is expected to adsorb on the surface of ZnO, and this strategy has a second advantage as the imine linkages of the resultant sensor (ZnO coated with an imine-linked receptor) may offer additional binding sites for the recognition of metal ions. There are several reports on the modification of electrochemical sensors by ZnO nanocomposites. Bijad et al. [7] developed ZnO/CNTs nanocomposite ionic liquid paste electrode as a sensitive voltammetric sensor for determination of ascorbic acid (AA) in food samples. Under the optimised conditions, the oxidation peak current of AA showed linear dynamic range 0.1–450 μmol L^{-1} with a detection limit of 0.07 μmol L^{-1}, using the DPV method.

Sadeghi et al. [8] developed a novel biosensor based on ZnO nanoparticle/1,3-dipropylimidazolium bromide ionic liquid-modified carbon paste electrode for square-wave voltammetric determination of epinephrine. The electrode was modified with zinc oxide (ZnO) nanoparticles which increased the oxidation peak current about three times at

Electronic supplementary material The online version of this article (doi:10.1007/s10800-014-0746-3) contains supplementary material, which is available to authorized users.

S. K. Mittal (✉) · R. Sharma · M. Sharma · M. Chhibber
School of Chemistry & Biochemistry, Thapar University, Patiala 147004, India
e-mail: smittal2001@yahoo.com; smittal@thapar.edu

N. Singh · J. Singh
Department of Chemistry, Indian Institute of Technology, Ropar 140001, Punjab, India

N. Kaur
Department of Nanoscience and Nanotechnology, Punjab University, Chandigarh 160014, India

the surface of IL/ZnO/NP/CPE compared to CPE. The linear response range and detection limit were found to be 0.09–800 and 0.06 μmol L^{-1}, respectively. Karimi–Maleh and co-workers [9] also developed a ZnO/CNTs nanocomposite/catechol derivative-modified electrode for liquid phase determination of glutathione and amoxicillin. Their square-wave voltammetric peak current increased linearly with their concentration at the ranges of 0.002–720 and 1.0–950 μM, respectively, with the detection limits of 0.0008 and 0.5 μM, respectively. Karimi–Maleh and co-workers [10] also developed an electrochemical nanocomposite-modified carbon paste electrode as a sensor for simultaneous determination of hydrazine and phenol in water and wastewater samples. Square-wave voltammetry (SWV) of hydrazine at the modified electrode exhibited two linear dynamic ranges with a detection limit (3σ) of 8.0 nmol L^{-1}.

Karimi–Maleh et al. [11] also developed a novel-modified carbon paste electrode based on NiO/CNTs nanocomposite and (9,10-dihydro-9,10-ethanoanthracene-11,12-dicarboximido)-4-ethylbenzene-1,2-diol as a mediator for simultaneous determination of cysteamine (CA), nicotinamide adenine dinucleotide (NADH) and folic acid (FA). Elyasi et al. [12] developed a highly sensitive voltammetric sensor based on Pt/CNTs nanocomposite-modified ionic liquid carbon paste electrode for determination of Sudan I in food samples. Karimi–Maleh et al. [13] explained the electrocatalytic and simultaneous determination of ascorbic acid, nicotinamide adenine dinucleotide, and folic acid at Ruthenium(II) Complex-ZnO/CNTs nanocomposite-modified carbon paste electrode with detection limits of 0.005, 0.5 and 1.0 mmol L^{-1}, respectively.

Kim et al. [14] developed an imine-based fluorescent chemosensor for the detection of aluminium in methanol–water. In this assay, aluminium could selectively participate in complex formation with the receptor, which resulted in a colour change and fluorescence enhancement. Sharma et al. [15] synthesised and developed fluorescent and chromogenic imine linked chemosensors (*T4* and *T5*) for the detection of aluminium. These receptors detect Al^{3+} using two different spectroscopic techniques. However, sensor *T5* detects aluminium on fluorescence through PET mechanism. Sharma et al. [16] developed a fluorescent chemosensor (*T6*) for the nanomolar detection of Co^{2+}.

The electrochemical methods are simple and reliable techniques for detecting metal ions. Furthermore, electroanalytical methods have some merits such as low detection limits, simple operation, portable equipments, low cost and fast over spectrometric methods. In this research work, ZnO-coated imine linkage-based chemosensors have been used for the determination of aluminium and cobalt ions.

There are several reported imine-based chemosensors used for metal determination. Noh et al. [17] developed an imine-based colorimetric and fluorescent chemosensor for cyanide detection in a 1:1 stoichiometric manner, which induces a fast colour change from colourless to orange and a dramatic enhancement in fluorescence intensity selectively for cyanide anions over other anions. Saluja et al. [18] developed an imine linked chemosensor for Mg^{2+} and fluorescent chemosensor for Cr^{3+}. The same sensor can be used to detect Mg^{2+} using UV-Vis absorption spectroscopy. Saluja et al. [19] developed a highly selective imine-based sensor, with a chelate ring consisting of –OH and sp^2 N moieties for the detection of zinc ions in an aqueous surfactant solution.

Reported methods for the detection of aluminium include atomic absorption spectrometry (AAS) [20], inductively coupled plasma atomic emission spectrometry (ICP-AES) [20] and ICP mass spectrometry (ICP-MS) [21] and fluorescent analysis [22]. Several methods are available to quantify cobalt ions including radiometrical, ICP-AES/OES, ICP-MS, electrochemical and spectrophotometric techniques [23–25]. The potentiometric technique has also been widely used for routine applications. However, sensitivity and detection limit of such methods is low. Moreover, these are often complicated, time-consuming, expensive and not used for routine applications [26–29]. Thus, the determination of aluminium and cobalt in environmental and biological system is of current interest and the development of a simple, reliable, and accurate method to determine trace level aluminium and cobalt is in great demand.

Till now, there is no report on imine-based voltammetric chemosensor for the detection of metal ions. So, in this research work, voltammetric sensors based on imine linkages are reported for the detection of aluminium and cobalt ions. *T4*, *T5* and *T6* have been synthesised using the literature method [15, 16] and then used for the determination of aluminium and cobalt ions by voltammetric methods. Results have been compared with other reported chemosensors (Table 1).

2 Experimental section

2.1 Synthesis and characterization

Organic receptors were synthesised as reported elsewhere [15, 16]. Synthesis of the molecules was confirmed with ^{1}H NMR data, as reported below:

2.1.1 Characterization by NMR Spectrometry

*2.1.1.1 ^{1}H NMR spectrum of **T4*** δ(ppm) 3.01 (t, 4H, $–CH_2$), 3.72 (t, 4H, $–CH_2$), 7.90 (S, 2H, Ar), 7.92 (d, 2H, Ar), 7.96 (d, 2H, Ar), 8.45 (s, 2H, –CH=N–), 9.57 (s, 2H, –OH).

*2.1.1.2 ^{1}H NMR spectrum of **T5*** δ(ppm) 2.95 (t, 4H, $–CH_2$), 3.62 (t, 4H, $–CH_2$), 6.79 (d, 2H, Ar), 7.15–7.40 (m, 4H, Ar), 7.50 (d, 2H, Ar), 7.60 (d, 2H, Ar), 7.77 (d, 2H, Ar), 8.69 (s, 2H, –CH=N–), 10.7 (s, 2H, –OH).

Table 1 Comparative study of imine-based chemosensors used with different techniques

S. no.	Receptors	Technique used	LOD	Interference	Reference
1	Juloidine-imidazole-based moiety	Colorimetric & Fluorescence	3.9 μM	Zn^{2+}, Ga^{3+}	[30]
2	1-[[(2-furanylmethyl)imino]methyl]-2-naphthol (1-*H*)	Fluorescence	6.03 μM	Cu^{2+},Fe^{3+}	[31]
3	o-Phenolsalicylimine	Colorimetric & Fluorescence	–	Ga^{3+}	[14]
4	Di(*O*-salicylaldimino-o-hydroxyphenyl)alkane	Potentiometry	100 μM	Ca^{2+}, Mg^{2+}	[32]
5	[1,2,5,6-tetraoxo- 3,4,7,8-tetraaza-(1,2,3,4,5,6,7,8) tetrabenzene(L)]	Cyclic voltammetry	–	Mn^{2+}, Cu^{2+}	[33]
6	2,2 -diphenyl-*N*,*N*-*bis*(2-pyridylmethylene)biphenyl-4,4-diamine	UV–Vis & Fluorescence	–	Mn^{2+}, Zn^{2+}, Zr^{4+}	[34]
7	*p*-(4-*n*-Butylphenylazo) calix [4] arene	Potentiometry	4.0 μM	Na^{+}, Zn^{2+}	[35]
8	***T4***, ***T5*** and ***T6***	CV, DPV & Potentiometry	0.42 μM	No interference	Present work

Table 2 Peak potentials (V) and peak currents (A) values for ***T4***, ***T5*** and ***T6***

Compound	Peak potentials (V)		Peak current (A)	
	E_{pc1}	E_{pc2}	i_{pc1}	i_{pc2}
T4	−0.930	−1.199	1.05×10^{-5}	1.63×10^{-5}
T5	−0.996	−1.850	1.56×10^{-5}	1.16×10^{-5}
T6	−1.220	–	5.23×10^{-6}	–

E_{pc} cathodic peak potential, i_{pc1} cathodic peak current

2.1.1.3 ^{1}H NMR spectrum of ***T6*** δ(ppm) 13.29 (bs, 2H, OH), 8.31 (s, 2H, N=CH), 7.23 (t, 2H, ArH), 7.18 (d, 2H, ArH), 6.91 (d, 2H, ArH), 6.82 (t, 2H, ArH), 3.67 (m, 4H=NCH_2), 2.95 (m, 4H, NCH_2)

2.1.2 Preparation of ZnO nanoparticle [15]

The ZnO was synthesised by mixing the alcoholic solution $Zn(NO_3)_2{\cdot}6H_2O$ (595 mg, 2.0 mmol) with alcoholic solution of NaOH (120 mg, 3.0 mmol). A white product was separated out and the product was washed with ethanol. The product was dried at 150 °C. The ZnO was characterised from X-ray diffraction pattern (Fig. S1). Further, SEM images of these receptors coupled with ZnO nanoparticle were characterised as shown in Figs. S2–S4.

2.2 Voltammetric study

2.2.1 Reagents

Solvents (acetonitrile, dichloromethane, dimethyl sulfoxide) used in the electrochemical experiments were of HPLC grade (Sd Fine, India) and used as obtained. Tetrabutylammonium perchlorate (Sigma Aldrich) was used as a supporting electrolyte in all the experiments. For cation interaction investigation, nitrate (Loba Chemie, India) and perchlorate salts (Sigma Aldrich) of the metal were used. Nitrogen gas was used for making the solution oxygen free. The compounds ***T4***, ***T5*** and ***T6*** were synthesised by our coworkers. These molecules have the following structures:

2.2.2 Instrumentation

All voltammograms were recorded using a three-electrode system immersed in a solution of the analyte species, supporting electrolyte in dry dimethyl sulfoxide on an Autolab Potentiostat/Galvanostat model PGSTAT12 (ECO Chemie, The Netherlands). The working electrode was a glassy carbon electrode (CH Instruments, USA, 3 mm diameter). The platinum electrode was used as a counter electrode. All the potentials were reported against Ag/Ag^{+} reference electrode. The Ag/Ag^{+} electrode contained an internal solution of 0.01 M $AgNO_3$ and 0.1 M TBAP in solvents like acetonitrile, dimethyl sulfoxide and dichloromethane. The working GC electrode was polished with alumina followed by washing with water and solvent before each cyclic voltammogram. The electrochemical measurements were carried out at a temperature of 25.0 ± 1 °C. In all experiments, the test solutions were de-aerated by a stream of N_2 gas purging through the solution for at least 4–5 min.

2.3 Potentiometric study

2.3.1 Reagents

Reagent grade o-nitrophenyl octyl ether (o-NPOE), sodium tetraphenylborate (NaTPB), tetrahydrofuran (THF) and high molecular weight PVC were purchased from Sigma Aldrich. Hydrated salts like $Al(NO_3)_3$, $Cu(NO_3)_2$, $Ca(NO_3)_2$, $Zn(NO_3)_2$, $Co(NO_3)_2$, $Mg(NO_3)_2$, $Fe_2(SO_4)_3$ (analytical grade) were purchased from Sigma Aldrich and were used as such. Salts like $Ce(NO_3)_3$, $Cr(NO_3)_3$, $Sm(NO_3)_3$, $Pr(NO_3)_3$,

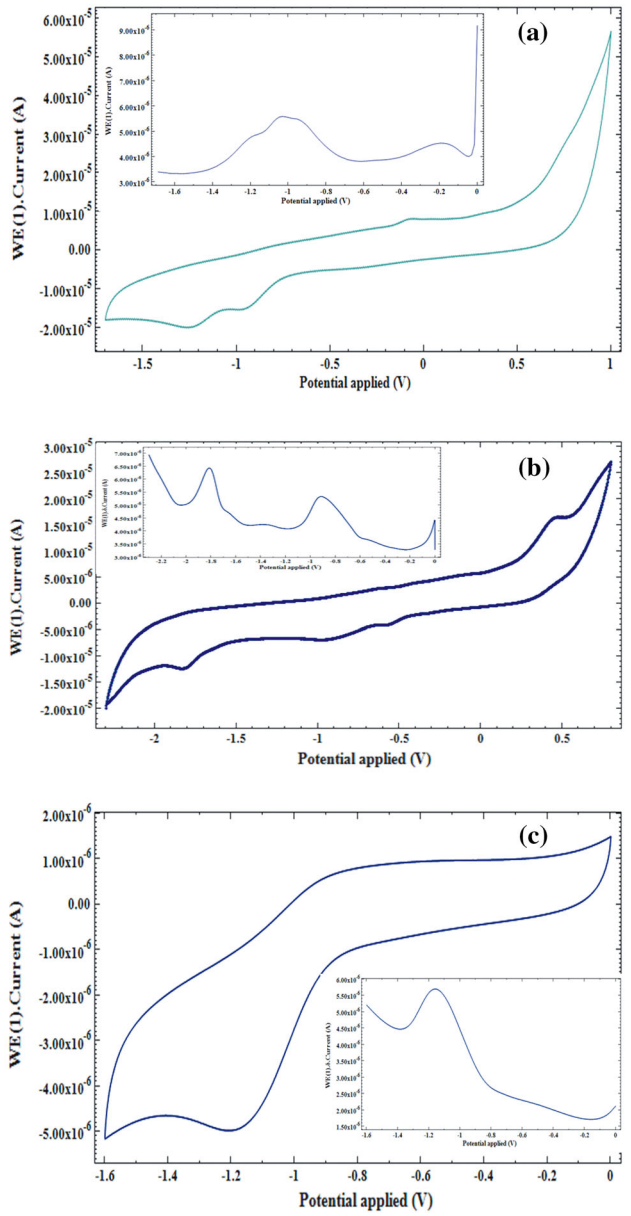

Fig. 1 Cyclic voltammograms of **a** ***T4*** **b** ***T5*** and **c** ***T6*** in DMSO:H_20 (8:2, v/v) (5×10^{-4} M). *Inset* DPV for **a** ***T4*** **b** ***T5*** and **c** ***T6*** Modulation amplitude 50mVsec^{-1}, (5×10^{-4} M)

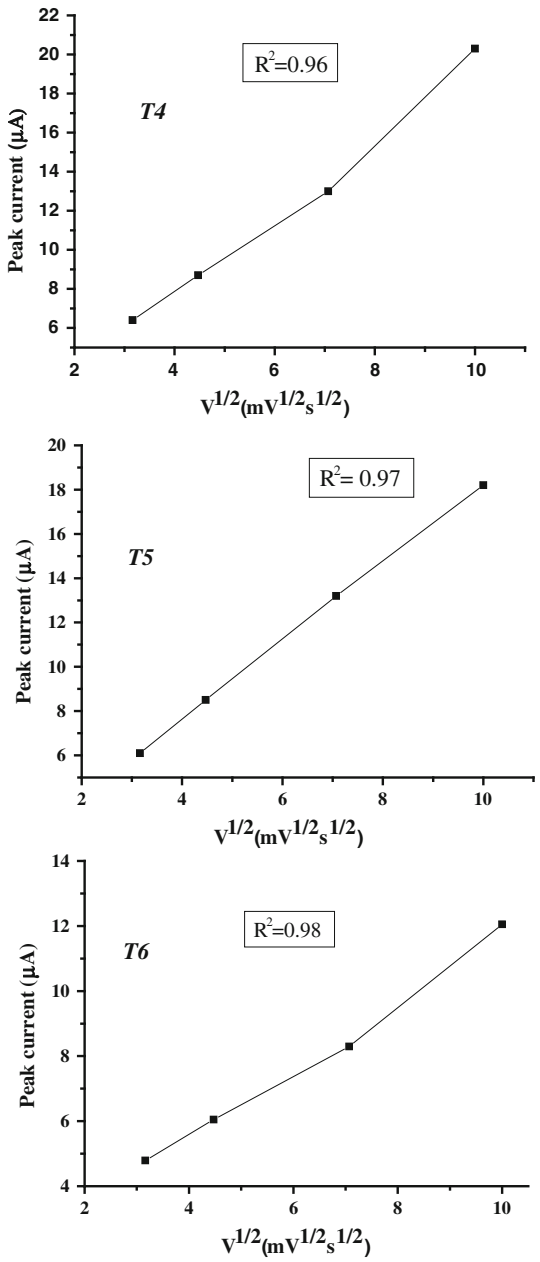

Fig. 2 Plots of peak current and square root of scan rate for ***T4***, ***T5*** and ***T6***

$Tb(NO_3)_3$, $La(NO_3)_3$, were purchased from CDH (central drug house, India). Doubly distilled deionised water was used throughout the experiments.

2.3.2 Membrane preparation and instrumentation

Six membranes with three different ionophores were prepared by standard procedure. PVC, o-NPOE, lipophilic salt and ionophores (T4, T5 and T6 without CNTs and with CNTs) were dissolved separately in THF at room temperature. Potentiometric measurements were made using digital potentiometer. All the measurements were done using the following cell assembly:

$$\mathrm{SCE}\left|\mathrm{Al}^{3+}/\mathrm{Co}^{2+}(0.1)\ \mathrm{M}\right|\left|\mathrm{Membrane}\right|\left|\ \mathrm{Al}^{3+}/\mathrm{Co}^{2+}(\mathrm{Test\ solution})\right|\mathrm{SCE}$$

2.4 Theoretical study

Density functional theory (DFT) calculations were carried out with the GAUSSIAN 03 W package. Optimization of the molecules was carried out using B3LYP/6-31G level of theory while metal complexation studies were carried out using LAN2DZ method using basis sets B3LYP/6-31G.

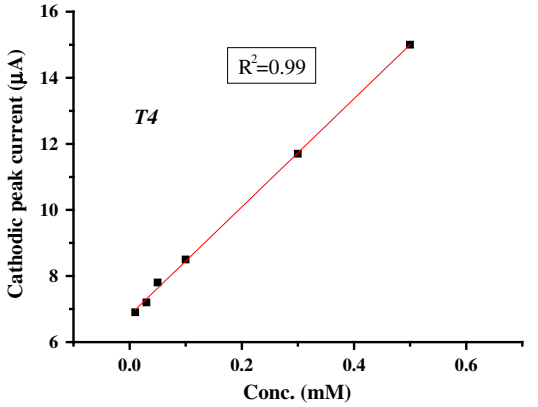

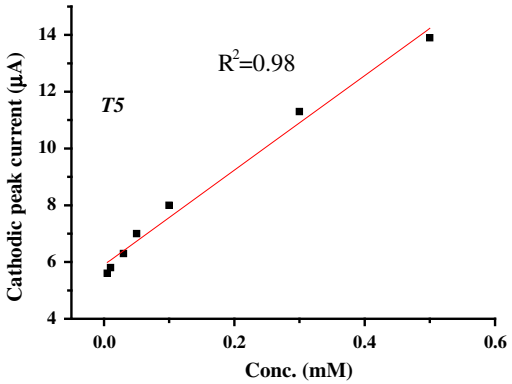

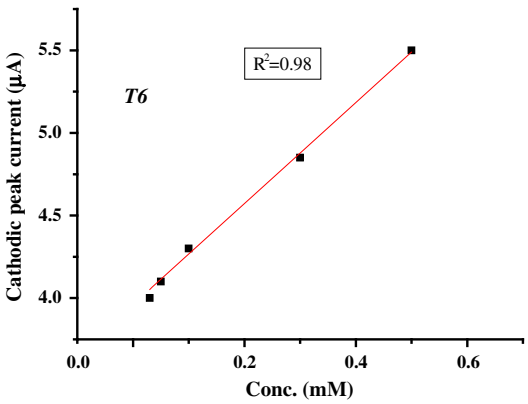

Fig. 3 Calibration curves of concentration of receptor and peak current for ***T4***, ***T5*** and ***T6***

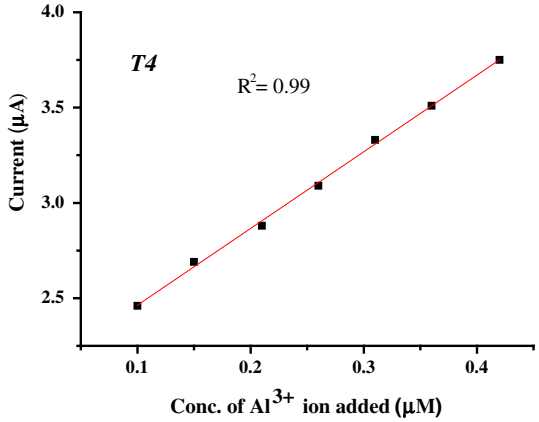

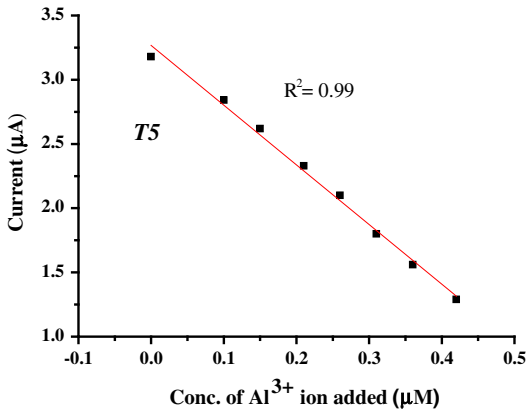

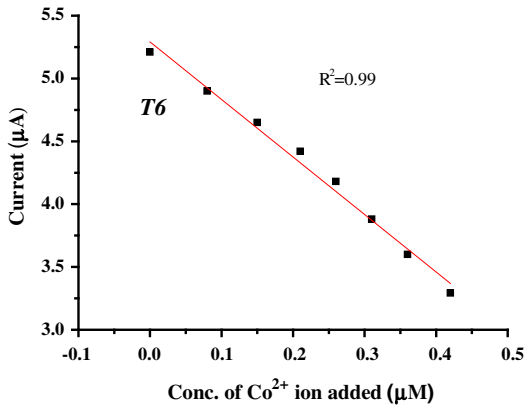

Fig. 4 Response of different concentrations of Al^{3+} for receptors ***T4*** & ***T5*** and of Co^{2+} for ***T6***

Table 3 Peak potentials of cathodic peak of ***T4***, ***T5*** and ***T6*** in different solvents

Solvent	Dipole moment (D)	E_{pc} (V)		
		T4	***T5***	***T6***
ACN	3.92	−1.212	−1.404	−1.454
DMSO	3.96	−0.998	−1.211	−1.261
DCM	1.60	–	–	–

E_{pc} cathodic peak potential

3 Results and discussion

3.1 Voltammetric study

*3.1.1 Electrochemical behaviour of **T4**, **T5** and **T6***

Cyclic voltammograms of ***T4*** and ***T5*** showed two reduction peaks each at −0.930, −1.199 and −0.996, −1.850 V, respectively, while ***T6*** showed one reduction peak (−1.220 V) as shown in Table 2. All the three chemosensors

Table 4 Peak potential (V) values for ***T4***, ***T5*** *and* ***T6*** alone and with different metal ions

Receptor with Metal ions (0.20 μM)	Peak potentials (V)									
	E_{pc1}			E_{pc2}		ΔE_{pc1}			ΔE_{pc2}	
	T4	***T5***	***T6***	***T4***	***T5***	***T4***	***T5***	***T6***	***T4***	***T5***
Receptor (without metal ion)	−0.902	−0.967	−1.205	−1.160	−1.810	–	–	–	–	–
With Mg^{2+}	−0.911	−0.977	−1.198	−1.162	−1.811	−0.009	−0.010	+0.007	−0.002	−0.001
With Ca^{2+}	−0.899	−0.962	−1.202	−1.201	−1.815	+0.003	+0.005	+0.003	−0.041	−0.005
With Na^{+}	−0.904	−0.969	−1.199	−1.112	−1.782	−0.002	−0.002	+0.006	+0.048	+0.028
With K^{+}	−0.912	−0.977	−1.203	−1.114	−1.785	−0.010	−0.010	+0.002	+0.046	+0.025
With Co^{2+}	−0.915	−0.979	–	−1.142	−1.801	−0.013	−0.012	–	+0.018	+0.009
With Al^{3+}	−0.648	–	−1.199	–	–	+0.254	–	+0.009	–	–

show peaks in cathodic region which vary in their respective peak potentials due to substituent effect. Peak at −1.199 V for ***T4*** was observed at −1.850 V for ***T5*** probably due to the presence of electron donating group (phenyl group) replacing nitro group of ***T4***. Phenyl group being electron donating as compared to nitro (an electron withdrawing group) makes reduction of imine double bond more difficult, hence shift of the cathodic peak to more negative potential (−1.850 V from −1.199 V), while no such substituent effect is present in ***T6,*** as there is no substituent on the phenyl ring and cathodic peak appears at −1.220 V. These observations are also supported by the DPV curves of the molecules (inset (a), (b) and (c) in Fig. 1).

3.1.2 *Influence of scan rate*

With increase in scan rate from 5 to 50 mVs^{-1} (Fig. S5), the voltammetric peak at −1.199 V disappears in ***T4***, probably an indication of two separate reduction reactions, out of which one reaction is very slow and cannot be recorded at a scan rate 50 mV s^{-1} or more. One of the two peaks for ***T4***, the one at −0.930 V was selected for quantitative studies on the basis of its reproducible behaviour. Unlike ***T4***, the corresponding peak in ***T5*** sustains fast scan but shifts to -1.85 V. This is due to the remote effect of substituent (NO_2 to Phenyl group) on the meta position to the electroactive centre (imine group) in the molecule. Peak currents of cathodic waves for ***T4***, ***T5*** and ***T6*** were plotted against square root of scan rates separately. A linear relation between peak current and the square root of scan rate indicated a diffusion-based process (Fig. 2).

3.1.3 *Effect of concentration of* ***T4, T5*** *and* ***T6***

Electrochemical study of the compounds was done to know the effect of different concentrations on their respective DPV behaviours. The results are shown in Fig. S6. With increase in concentration of each of ***T4***, ***T5*** and ***T6***, increase in the respective peak currents was observed along with a cathodic shift in the peak potential. This is due to the reason that increase in concentration makes the velocity of mass diffusion rapid and hence the electrode processes are more controlled by the electrode kinetics. Calibrations for concentration of analyte species and cathodic peak currents were plotted and the coefficient of regression varies within a range 0.98–0.99 as shown in Fig. 3.

3.1.4 *Effect of solvent*

Voltammetric scans of ***T4*** were studied in different solvent systems like ACN, DMSO and DCM (Fig. S7). The solvents were selected in such a way that their electron donating tendencies (Lewis basicity) were significantly different. As expected, ACN influenced reduction of imine bond in ***T4*** molecule more than DMSO because of more basic character of lone pair on nitrogen atom of ACN resulting in increase in electron density of imine bond in ***T4*** as compared to that of oxygen in DMSO. This is indicated from greater peak potential (−1.212 V) in ACN as compared to peak potential (−0.998 V) in DMSO as a solvent, while DCM did not give good curves.

Experiments were also conducted in solvent: H_2O mixtures taken in 8: 2 ratios (Fig. S8). Presence of H_2O in DMSO resulted in significant shift (0.214 V) in cathodic peak potential from −0.998 to −1.212 V. This is because of H_2O being more basic in character as compared to DMSO, which further strengthens electron cloud over imine bond and hence resulting in a significant positive shift in cathodic peak potential.

In case of ACN:H_2O mixture, trend in shift is reversed as basicity of H_2O is much lower than that of ACN. So, replacement of 20 % of ACN with H_2O molecules results in significant shift of cathodic peak potential from −1.212 to −0.910 V. Because of immiscibility of DCM in aqueous

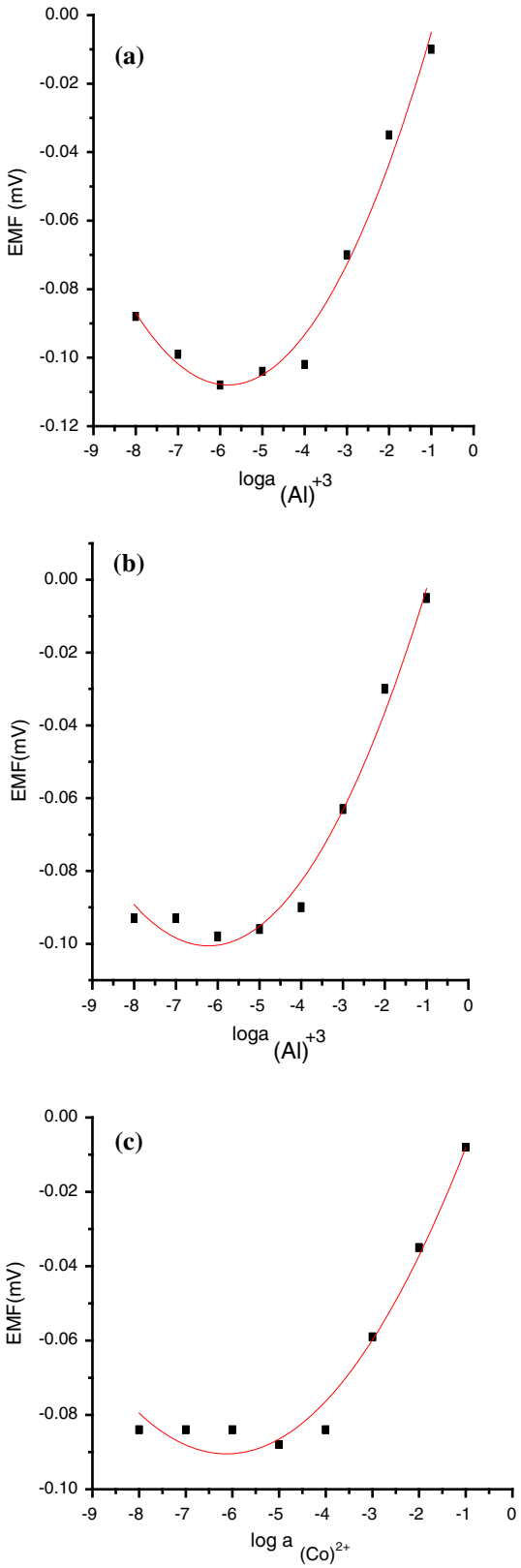

Fig. 5 Calibration curves for Al^{3+}/Co^{2+} ions using electrode with **a** Ionophore ***T4***, **b** Ionophore ***T5*** and **c** Ionophore ***T6***

medium, it did not give discrete bands or peaks. These results have also been observed in differential pulse voltammetry as well. For all the three molecules, trends of voltammograms are the same as the electroactive site in all of these is an imine bond. Studies of solvent effect on voltammograms of molecules ***T5*** and ***T6*** indicate that trends of peak potentials were same as for ***T4*** molecule. Voltammograms are given in Fig. S9. A complete record of peak potentials and shifts for all the molecules ***T4***, ***T5*** and ***T6*** are given in Table 3.

*3.1.5 Electrochemical recognition of metal ions by **T4**, **T5** and **T6***

Experiments were conducted with different metal ions like Co^{2+}, Mg^{2+}, Ca^{2+}, Na^{+}, K^{+} and Al^{3+} in DMSO:H_2O (8:2, v/v) at a scan rate of 20 mV s^{-1} to understand complexation behaviour of ***T4***, ***T5*** and ***T6*** with metal ions. In the presence of Al^{3+} ions, shapes of voltammograms of ***T4*** and ***T5*** are different from those of ***T6*** (Fig. S10) which shows a decrease in peak current at peak potential −1.205 V in presence of Co^{2+} ions. Voltammogram for Al^{3+}***–T4*** complex showed an additional peak at −0.648 V, as shown in Fig. S11. A detailed study was done with different concentrations of metal ions ranging from 0.0 μM to 0.42 μM of the ***T4***, ***T5*** and ***T6***.

*3.1.5.1 Voltammograms of **T4*** In voltammogram of ***T4*** (Fig. S11), intensity of the cathodic peak at -1.160 V (1.72×10^{-5} A for 0.30 μM) decreases with increase in concentration of Al^{3+} ions and gets diminished at 0.10 μM of the metal ion. With further increase in concentration of the metal ion from 0.10 to 0.42 μM, a new cathodic peak emerges at −0.648 V, due to the formation of metal–ligand complex. Before this concentration of the new peak was not visible probably due to instability of the complex. An almost linear change in cathodic peak current was observed (for peak at −0.648 V) for different concentrations indicating a quantitative response of ***T4*** for Al^{3+} ions (Fig. 4).

On gradual addition of Al^{3+} ions, the current magnitude increases because of the electroactive nature of the complex. On complexation with Al^{3+} ions, a cathodic shift of about 0.254 V in the cathodic peak potential of ***T4*** was observed while in presence of other metal ions (listed as, Table 4) a shift of 0.002–0.013 V was recorded and their peak currents remain almost same even at high concentrations of different metal ions. This indifference in peak currents in the presence of metal ions other than Al^{3+}, indicates that ***T4*** is more selective towards Al^{3+} ions.

A tentative selectivity order for metal ions in case of ***T4*** based on shift in peak potential at −0.902 V can be written as:

Table 5 Slopes of the calibration curves and detection limits (DL) by calibration curves for Al^{3+}/Co^{2+} ions using electrodes with ***T4***, ***T5*** and ***T6***

Slope (mV) and detection limit (ML^{-1})										
S. no.	Ionophore *T4*		Ionophore *T5*		Ionophore *T6*		Ionophore *T4* with CNTs		Ionophore *T5* with CNTs		Ionophore *T6* with CNTs	
	Slope	DL	Slope	DL	Slope	DL	Slope	DL	Slope	DL	Slope	DL
1	17.0	2×10^{-5}	16.5	1×10^{-5}	19.0	1×10^{-5}	16.5	1×10^{-6}	18.0	6×10^{-5}	22.0	5×10^{-5}
2	18.0		17.5		22.0		18.0		19.0		19.0	
3	16.5		17.0		17.0		18.0		16.3		19.0	
4	18.0		19.0		19.5		19.0		19.4		17.0	
Mean	17.3 ± 1.0		17.5 ± 1.5		19.3 ± 1.0		17.8 ± 2.0		18.1 ± 1.0		19.3 ± 2.0	

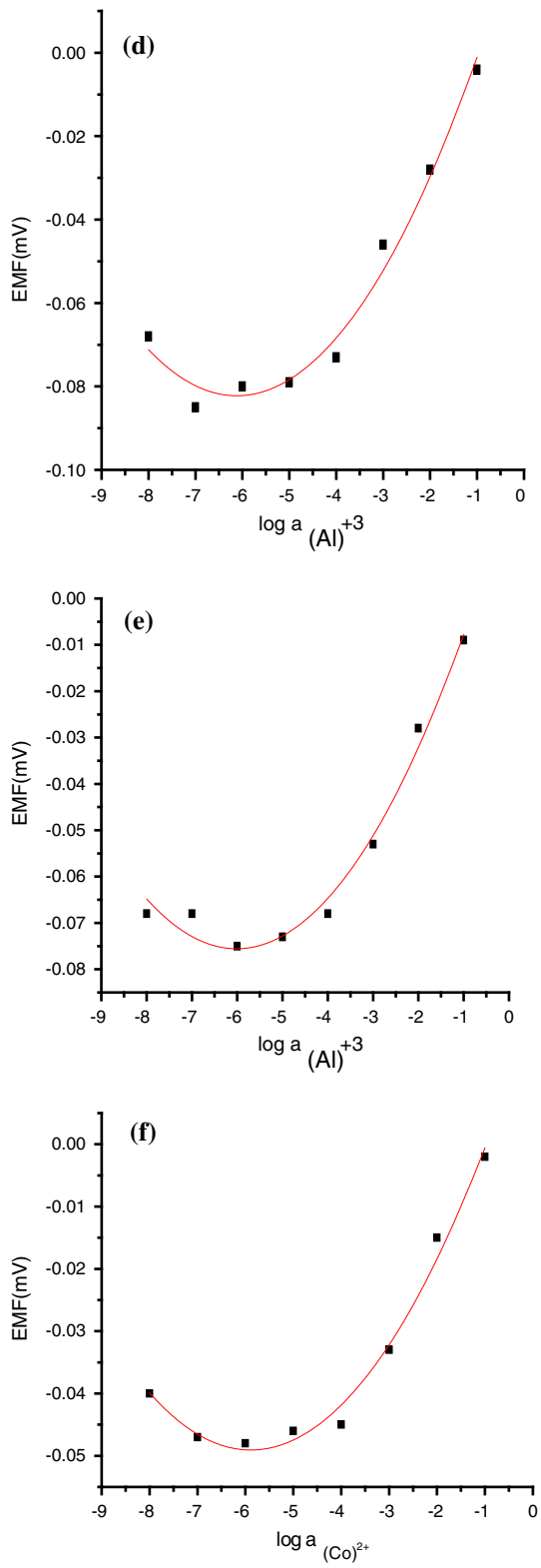

Fig. 6 Calibration curves for Al^{3+}/Co^{2+} ion using electrode with **d** Ionophore ***T4*** with CNTs, **e** Ionophore ***T5*** with CNTs and **f** Ionophore ***T6*** with CNTs

$Al^{3+} \gg > Ca^{2+} > Na^{+} > Mg^{2+} > K^{+} > Co^{2+}$

3.1.5.2 Voltammograms of ***T5*** In voltammogram of ***T5*** (Fig. S11), intensity of the cathodic peaks at −1.810 and −0.967 V decreases with increase in concentration of Al^{3+} ions and gets fully diminished at 0.42 μM. An almost linear change in cathodic peak current was observed for different concentrations indicating a quantitative response of ***T5*** for Al^{3+} ions (Fig. 4). In presence of other metal ions (listed as, Table 4), a shift of 0.001–0.028 V was recorded and their peak currents remained almost same even at high concentration. This indifference of peak current in the presence of metal ions other than Al^{3+} indicates that ***T5*** is more selective towards Al^{3+} ions.

Based on shifts in peak potentials in presence of different metal ions, a tentative selectivity order for metal ions can be written as:

$Al^{3+} \gg > Ca^{2+} > Na^{+} > Mg^{2} \approx K^{+} > Co^{2+}$

3.1.5.3 Voltammograms of ***T6*** In voltammogram of ***T6*** (Fig. S11), intensity of the cathodic peak at -1.205 V decreases with increase in concentration of Co^{2+} ions and gets diminished at 0.42 μM of the metal ion. A change in cathodic peak current was observed for different concentrations indicating a quantitative response of ***T6*** for Co^{2+} ions (Fig. 4). In presence of other metal ions (listed as, Table 4), a shift of 0.001–0.009 V was recorded and their peak currents remained almost same even at higher concentrations of metal ions. This indifference of peak current in the presence of metal ions other than Co^{2+} indicated that ***T6*** is more selective towards Co^{2+} ions.

Based on shifts in peak potentials of ***T6***, a tentative selectivity order for metal ions can be written as:

$Co^{2+} \gg > Al^{3+} > Mg^{2+} > Na^{+} > Mg^{2+} > Ca^{2+} > K^{+}$

3.2 Potentiometric study

PVC membrane electrodes containing receptors ***T4***, ***T5*** and ***T6*** were equilibrated separately with $Al(NO_3)_3$ and $Co(NO_3)_2$ for about 5 days so as to saturate the cavities of receptors (***T4*** and ***T5***) with aluminium ions and receptor (***T6***) with cobalt ions. Potentiometric readings were recorded with the electrode immersed in the different concentration of aluminium ion/cobalt ion as the primary ion in the concentration range of 10^{-8} to 10^{-1} M. Electrode potentials were plotted against concentration of the metal ion to draw calibration curves (Fig. 5).

Slopes of calibration curves for Al^{3+}/Co^{2+} ion using electrode with receptors i.e. T4, T5, T6 without CNTs and with CNTs, were calculated and given in Table 5. From the graphs (Fig. 6), it is observed that all the electrodes with receptors exhibited near Nernstian slopes with working range from 10^{-5} to 10^{-1}.

3.2.1 Interference studies

Effect of interfering ions on the potentiometric response of the electrode was measured by fixed interference method. Concentration of the primary ion was varied from 10^{-8} to 10^{-1} M but the concentration of the interfering ion was fixed i.e., 10^{-3} M. The selectivity coefficient values of Al^{3+} selective electrode prepared with receptors ***T4***, ***T5***, ***T6*** for different interfering ion are shown in Table 6.

For membranes with CNTs, interference studies were done in the same way as with electrodes without CNTs. It can be concluded from the values of selectivity coefficients (Table 6) that ions having values less than one show limited interference with the working of the proposed electrode for Al^{3+}/Co^{2+}determination. The electrodes show reasonably good selectivity for aluminium ion in the presence Fe^{3+}, Cr^{3+}, Tb^{3+}, Sm^{3+}, La^{3+} and Ce^{3+} while it suffers interference from Co^{2+}, Zn^{2+}, Cu^{2+}, Mg^{2+} and Ca^{2+}. The membrane electrodes containing CNTs in the matrix along with the ionophore did not show much difference in their performance except for a little less interference from the above listed metal ions.

3.2.2 Effect of pH

pH response of the electrode was studied by the use of 1×10^{-4} M Al^{3+} and Co^{2+}solution over pH range 2–10. Adjustment of pH was done by the drop wise addition of 10^{-1} M HNO_3 or 10^{-1} M NaOH solution to the test solution. Graphs of electrode potential (E) against pH of electrode with different ionophores are shown in Fig. 7.

Potential remains stable in different pH ranges for different receptors. The working pH range for electrodes with CNTs shows better pH range than those without CNTs.

Table 6 Selectivity coefficient values of Al^{3+}/Co^{2+} selective electrodes prepared with ***T4***, ***T5*** and ***T6***

S. no.	Interfering ions	Selectivity coefficient, log *K*		
		T4	*T5*	*T6*
1	Mg^{2+}	−0.04	0.39	−0.15
2	Zn^{2+}	0.44	0.54	0.30
3	Cu^{2+}	1.43	1.15	1.18
4	Ca^{2+}	0.30	0.69	0.59
5	Fe^{3+}	−2.21	−1.10	−1.60
6	Cr^{3+}	−0.80	−1.13	−1.61
7	Tb^{3+}	−1.50	−1.39	−1.50
8	Pr^{3+}	−1.51	−2.52	−1.73
9	Sm^{3+}	−1.22	−1.69	−1.37
10	La^{3+}	−0.89	−2.39	−1.38
11	Ce^{3+}	−1.19	−1.60	−1.52

Thus, the corresponding ranges are considered as the working pH range of the electrode.

3.3 Theoretical study

Energy contents of HOMO for molecules ***T4***, ***T5*** and ***T6*** have been recorded as −0.234, −0.068 and −0.227 eV; with their respective LUMO values as −0.114, −0.137 and −0.125 eV. The energy gaps for transition of electrons from highest occupied and lowest unoccupied molecular orbitals are observed as −0.120, −0.069 and −0.012 eV, respectively. It is quite interesting to observe that on bringing aluminium (for ***T4*** and ***T5***)/cobalt (for ***T6***) ions in the vicinity of each of these molecules, energy gap has reduced dramatically to 0.011 eV indicating greater stability of the ionophores in complexed form. Similar

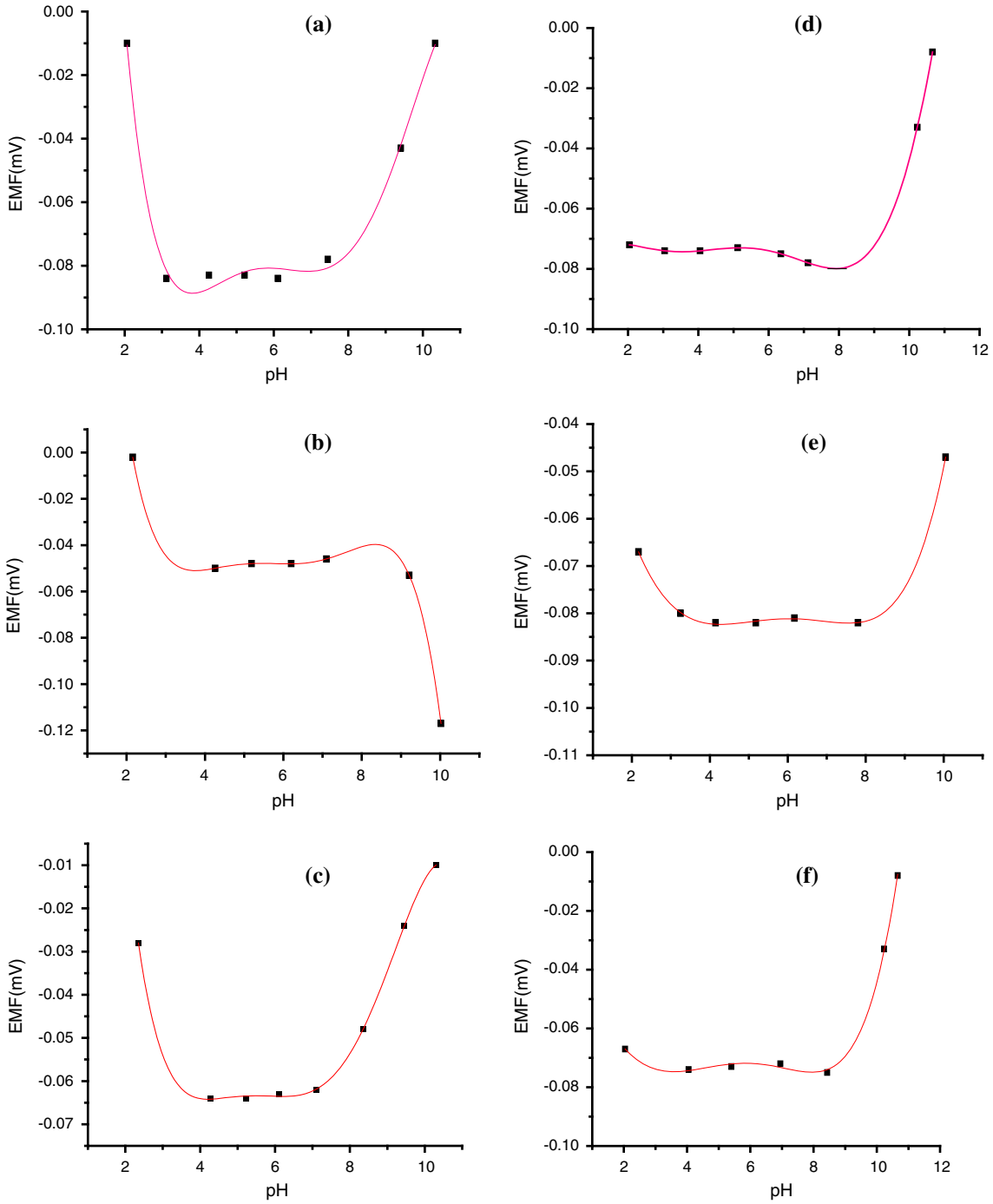

Fig. 7 Working pH range of electrodes with **a** Ionophore ***T4***, **b** Ionophore ***T5***, **c** Ionophore ***T6***, **d** Ionophore ***T4*** with CNTs with **e** Ionophore ***T5*** with CNTs and **f** Ionophore ***T6*** with CNTs

Table 7 Energy values (in eV) of HOMO, LUMO and LUMO+1 for ***T4***, ***T5*** and ***T6*** and their complexes with Al^{3+} and Co^{2+}

Molecule	Energy (eV)				
	E_{HOMO}	E_{LUMO}	E_{LUMO+1}	E_{gap1}	E_{gap2}
T4	−0.234	−0.114	−0.099	−0.120	−0.135
***T4*–Al^{3+}**	−0.531	−0.520	−0.455	−0.011	−0.076
T5	−0.068	−0.137	0.162	−0.069	−0.230
***T5*–Al^{3+}**	−0.482	−0.471	−0.394	−0.011	−0.088
T6	−0.227	−0.125	−0.083	−0.102	−0.144
***T6*–Co^{2+}**	−0.424	−0.412	−0.361	−0.012	−0.063

observations are repeated for energy gaps between E_{HOMO} and E_{LUMO+1} confirming stability of the molecules in presence of respective metal ions as shown in Table 7.

Electronic display of electron density through optimised geometries of ***T4***, ***T5*** and ***T6*** (Fig. 8) using Gaussian 03 W software and setting the basis sets as B3LYP/6-31G also indicate shift in electron clouds from ZnO particles electrostatically bonded to hydroxyl groups of the ionophore to the electron cloud spread over imine bond conjugated to benzene ring Fig. S12. The electron cloud of uncomplexed ***T6*** molecule gets stabilised after complexation with metal ion as observed from shift in electron cloud in Fig. S12.

In case of ***T4***, the electron clouds in distribution of HOMO stay on the molecule probably due to steric reasons while in ***T5*** the electron clouds move from ZnO region to benzene rings indicating more spread of the charge over molecule hence providing stability in presence of aluminium ion (as shown in Fig. S12).

From theoretical study, it can be concluded that stabilization of complexation of ***T4*** is more than that of ***T5*** in presence of aluminium ion based on E_{gap2} values. ***T6*–Co^{2+}** complexation provides still more stability than that of ***T4*** and ***T5*** with Al^{3+}.

3.4 Real-time sample analysis

T4, T5 *and* ***T6***-based chemosensors were tested for the analysis of real-time samples taken from the laboratory waste water drain. Each sample was spiked with the addition of 1 mL of 10^{-2} M standard metal ion solution, keeping the total volume of the sample equal to 100 mL.

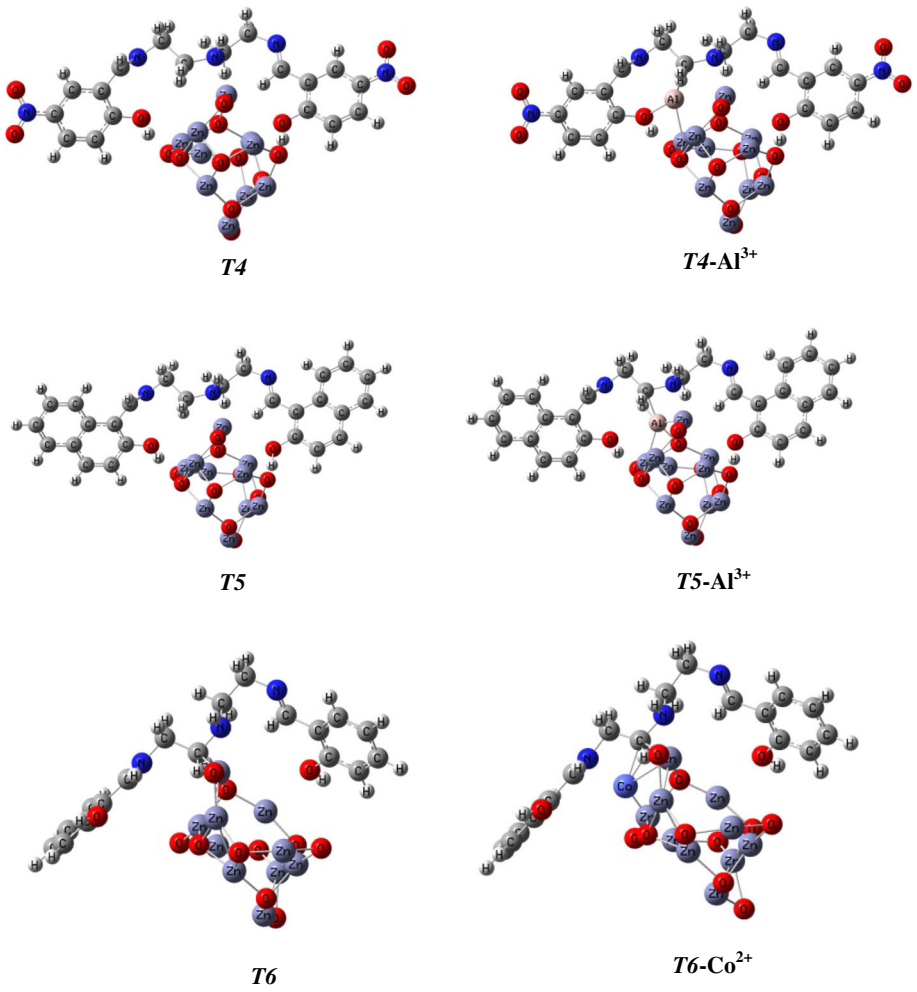

Fig. 8 Optimised geometries of ***T4***, ***T5*** and ***T6*** at B3LYP/6-31G level; ***T4*–Al^{3+}**, ***T5*–Al^{3+}** and ***T6*–Co^{2+}** complexation at B3LYP/LAN2DZ level using Gaussian 03W software

Table 8 Real-time sample analysis of laboratory drain waste water samples and its verification with complexometric method (n = 3)

Sample name	Al^{3+} conc. (10^7)		Al^{3+} conc. (10^7)		Co^{2+} conc. (10^7)	
	T4	Complexometric method	*T5*	Complexometric method	*T6*	Complexometric method
SM-1	12.57 ± 0.02	12.6 ± 0.1	12.59 ± 0.02	12.5 ± 0.5	13.29±0.03	13.3 ± 0.1
SM-2	21.71 ± 0.09	21.7 ± 0.1	22.59 ± 0.07	22.6 ± 0.2	17.59±0.09	17.6 ± 0.3
SM-3	20.19 ± 0.01	20.1 ± 0.2	19.89 ± 0.06	19.9 ± 0.2	18.59 ± 0.01	18.6 ± 0.4
SM-4	21.59 ± 0.07	21.5 ± 0.1	20.79 ± 0.05	20.7 ± 0.2	20.19 ± 0.04	20.2 ± 0.2
SM-5	15.69 ± 0.09	15.5 ± 0.3	14.89 ± 0.05	14.9 ± 0.1	14.61±0.03	14.5 ± 0.2

± Shows the standard deviation (n = 3)

The results obtained were verified using complexometric method as a reference method for the determination of heavy metal ions. Table 8 shows that the results obtained by the chemosensors are in complete agreement with the results obtained with complexometric method.

4 Conclusions

Imine-bridged receptors coupled with ZnO nanoparticles (***T4***, ***T5*** and ***T6***) formulate a cavity just suitable to hold reversibly metal ions like Al^{3+} and Co^{2+}. Behaviour of these molecules was studied both by voltammetric and potentiometric methods. Different substituents on the phenyl ring resulted in changing electronic environment in the cavity, experienced in the form of selectivity for the target metal ions. Interestingly, the observations are supported sufficiently with energy minimised conformations of the complexed receptors with target metal ions.

Response characteristics of the proposed molecules were supported by theoretical studies as well. While ***T4*** and ***T5*** responded selectively for aluminium ions in partially aqueous medium, ***T6*** responded equally well for cobalt ions as evident from the linear regression coefficients in the range 0.99–0.98 over a reasonably wide concentration range up to 0.42 μM of the metal ions. Presence of interfering metal ions like Na^+, K^+, Mg^{2+}, Ca^{2+}, Co^{2+} (in case of T4 & T5) and Al^{3+} (in case of T6) did not show any effect on the peak potential and high selectivity can be assigned to their respective complexing metal ions (Al^{3+} for ***T4*** & ***T5***, Co^{2+} for ***T6***). Differential pulse voltammetric studies on all the three complexing systems supported observations from cyclic voltammetric data. Potentiometric studies also supported well the results. Theoretical studies explained the stability of ***T4***–Al^{3+}, ***T5***–Al^{3+} and ***T6***–Co^{2+} complexes. The proposed analytical method has been validated with complexometric method for heavy metal detection in real-time samples.

Acknowledgments The authors are thankful to Thapar University, Patiala, for providing research facilities. Fruitful discussions with Dr. Narinder Singh of IIT Ropar, are gratefully acknowledged.

References

1. Olowu RA, Ndangili PM, Baleg AA, Ikpo CO, Njomo N, Baker P, Iwuoha E (2011) Spectroelectrochemical dynamics of dendritic poly (propylene imine)-polythiophene star copolymer aptameric 17β-estradiol biosensor. Int J Electrochem Sci 6:1686–1708
2. Bui N-N, Hong J-T, S-i Mho, Jang H-Y (2008) A ferrocene derivative redox sensor for mercuric ion: synthesis and electrochemical study. Notes 29(7):1395
3. Sutcliffe OB, Chesney A, Bryce MR (2001) Voltammetric metal cation sensors based on ferrocene derivatives with oxazoline and imine substituents. J Organomet Chem 637:134–138
4. Straumal BB, Myatiev A, Straumal P, Mazilkin A, Protasova S, Goering E, Baretzky B (2010) Grain boundary layers in nanocrystalline ferromagnetic zinc oxide. JETP Lett 92(6):396–400
5. Straumal BB, Protasova S, Mazilkin A, Schütz G, Goering E, Baretzky B, Straumal P (2013) Ferromagnetism of zinc oxide nanograined films. JETP Lett 97(6):367–377
6. Sharma H, Kaur N, Pandiyan T, Singh N (2012) Surface decoration of ZnO nanoparticles: a new strategy to fine tune the recognition properties of imine linked receptor. Sens Actuat B 166:467–472
7. Bijad M, Karimi-Maleh H, Khalilzadeh MA (2013) Application of ZnO/CNTs nanocomposite ionic liquid paste electrode as a sensitive voltammetric sensor for determination of ascorbic acid in food samples. Food Anal Methods 6(6):1639–1647
8. Sadeghi R, Karimi-Maleh H, Bahari A, Taghavi M (2013) A novel biosensor based on ZnO nanoparticle/1, 3-dipropylimidazolium bromide ionic liquid-modified carbon paste electrode for square-wave voltammetric determination of epinephrine. Phys Chem Liq 51(6):704–714
9. Karimi-Maleh H, Tahernejad-Javazmi F, Gupta VK, Ahmar H, Asadi MH (2014) A novel biosensor for liquid phase determination of glutathione and amoxicillin in biological and pharmaceutical samples using a ZnO/CNTs nanocomposite/catechol derivative modified electrode. J Mol Liq 196:258–263
10. Karimi-Maleh H, Moazampour M, Ensafi AA, Mallakpour S, Hatami M (2014) An electrochemical nanocomposite modified carbon paste electrode as a sensor for simultaneous determination of hydrazine and phenol in water and wastewater samples. Environ Sci Pollut Res 21(9):5879–5888

11. Karimi-Maleh H, Biparva P, Hatami M (2013) A novel modified carbon paste electrode based on NiO/CNTs nanocomposite and (9, 10-dihydro-9, 10-ethanoanthracene-11, 12-dicarboximido)-4-ethylbenzene-1, 2-diol as a mediator for simultaneous determination of cysteamine, nicotinamide adenine dinucleotide and folic acid. Biosens Bioelectron 48:270–275
12. Elyasi M, Khalilzadeh MA, Karimi-Maleh H (2013) High sensitive voltammetric sensor based on Pt/CNTs nanocomposite modified ionic liquid carbon paste electrode for determination of Sudan I in food samples. Food chem 141(4):4311–4317
13. Karimi-Maleh H, Tahernejad-Javazmi F, Daryanavard M, Hadadzadeh H, Ensafi AA, Abbasghorbani M (2014) Electrocatalytic and simultaneous determination of ascorbic acid, nicotinamide adenine dinucleotide and folic acid at Ruthenium (II) complex-ZnO/CNTs nanocomposite modified carbon paste electrode. Electroanalysis 26(5):962–970
14. Kim S, Noh JY, Kim KY, Kim JH, Kang HK, Nam S-W, Kim SH, Park S, Kim C, Kim J (2012) Salicylimine-based fluorescent chemosensor for aluminum ions and application to bioimaging. Inorg chem 51(6):3597–3602
15. Sharma H, Narang K, Singh N, Kaur N (2012) Imine linked chemosensors coupled with ZnO: Fluorescent and chromogenic detection of Al^{3+}. Mater Lett 84:104–106
16. Sharma H, Singh A, Kaur N, Singh N (2013) ZnO-based imine-linked coupled biocompatible chemosensor for nanomolar detection of Co^{2+}. ACS Sustain Chem Eng 1(12):1600–1608
17. Noh JY, Hwang IH, Kim H, Song EJ, Kim KB, Kim C (2013) Salicylimine-based colorimetric and fluorescent chemosensor for selective detection of cyanide in aqueous buffer. Bull Korean Chem Soc 34(7):1985
18. Saluja P, Kaur N, Kang J, Singh N, Jang DO (2013) Benzimidazole-based chromogenic chemosensor for the recognition of oxalic acid via counter ion displacement assay in semi-aqueous medium. Tetrahedron 69(43):9001–9006
19. Saluja P, Bhardwaj VK, Pandiyan T, Kaur S, Kaur N, Singh N (2014) Imine-linked chemosensors for the detection of Zn^{2+} in biological samples. RSC Adv 4(19):9784–9790
20. Chappuis P, Poupon J, Rousselet F (1992) A sequential and simple determination of zinc, copper and aluminium in blood samples by inductively coupled plasma atomic emission spectrometry. Clin Chim Acta 206(3):155–165
21. Melnyk LJ, Morgan JN, Fernando R, Pellizzari ED, Akinbo O (2003) Determination of metals in composite diet samples by inductively coupled plasma-mass spectrometry. J AOAC Int 86(2):439–447
22. Wang H, Yu Z, Wang Z, Hao H, Chen Y, Wan P (2011) Preparation of a preplated bismuth film on Pt electrode and its application for determination of trace aluminum(III) by adsorptive stripping voltammetry. Electroanalysis 23(5):1095–1099
23. Wiley B, Sun Y, Xia Y (2007) Synthesis of silver nanostructures with controlled shapes and properties. Acc Chem Res 40(10): 1067–1076
24. Chen H, Yuan F, Xu J, Zhang Y, Wu Y, Wang L (2013) Simple and sensitive detection method for Cobalt (II) in water using $CePO^4$: Tb^{3+} nanocrystals as fluorescent probes. Spectrochim Acta Part A Mol Biomol Spectrosc 107:151–155
25. Wang Y, Luo X, Tang J, Hu X, Xu Q, Yang C (2012) Extraction and preconcentration of trace levels of cobalt using functionalized magnetic nanoparticles in a sequential injection lab-on-valve system with detection by electrothermal atomic absorption spectrometry. Anal Chim Acta 713:92–96
26. Awual MR, Ismael M, Yaita T (2014) Efficient detection and extraction of cobalt (II) from lithium ion batteries and wastewater by novel composite adsorbent. Sens Actuat B 191:9–18
27. Awual MR, Yaita T, Okamoto Y (2014) A novel ligand based dual conjugate adsorbent for cobalt(II) and copper(II) ions capturing from water. Chemical, Sens Actuat B
28. Zhang X, Zhou Q, Lv Y, Wu L, Hou X (2010) Ultrasensitive determination of cobalt in single hair by capillary electrophoresis using chemiluminescence detector. Microchem J 95(1):80–84
29. Saifuddin N, Raziah A, Junizah A (2012) Carbon nanotubes: a review on structure and their interaction with proteins. J Chem 2013:1–18
30. Choi YW, Park GJ, Na YJ, Jo HY, Lee SA, You GR, Kim C (2014) A single schiff base molecule for recognizing multiple metal ions: a fluorescence sensor for Zn (II) and Al(III) and colorimetric sensor for Fe(II) and Fe(III). Sensors and Actuators B: Chemical 194:343–352
31. Sen S, Mukherjee T, Chattopadhyay B, Moirangthem A, Basu A, Marek J, Chattopadhyay P (2012) A water soluble Al^{3+} selective colorimetric and fluorescent turn-on chemosensor and its application in living cell imaging. Analyst 137(17):3975–3981
32. Gupta VK, Singh A, Ganjali M, Norouzi P, Faridbod F, Mergu N (2013) Comparative study of colorimetric sensors based on newly synthesized Schiff bases. Sensors and Actuators B: Chemical 182:642–651
33. Chandra S (2013) Synthesis, spectroscopic characterization, molecular modeling and antimicrobial activities of Mn(II), Co(II), Ni(II), Cu(II) complexes containing the tetradentate aza Schiff base ligand. Spectrochim Acta Part A Mol Biomol Spectrosc 103:338–348
34. Xu H, Tao X, Li Y, Shen Y, Wei Y (2012) Synthesis, characterization and metal ion-sensing properties of two Schiff base derivatives. Spectrochim Acta Part A Mol Biomol Spectrosc 91:375–382
35. Kumar P, Shim Y-B (2009) A novel cobalt (II)-selective potentiometric sensor based on *p*-(4-*n*-butylphenylazo) calix[4] arene. Talanta 77(3):1057–1062